Tilt, Twist, and Coiling in β-Barrel Membrane Proteins: Relation to Infrared Dichroism

Tibor Páli*† and Derek Marsh*
*Max-Planck-Institut für biophysikalische Chemie, Abteilung Spektroskopie, 37070 Göttingen, Germany; and the †Institute of Biophysics, Biological Research Center, 6701 Szeged, Hungary

ABSTRACT The x-ray coordinates of β-barrel transmembrane proteins from the porins superfamily and relatives are used to calculate the mean tilt of the β-strands and their mean local twist and coiling angles. The 13 proteins examined correspond to β-barrels with 8 to 22 strands, and shear numbers ranging from 8 to 24. The results are compared with predictions from the model of Murzin, Lesk, and Chothia for symmetrical regular barrels. Good agreement is found for the mean strand tilt, but the twist angles are smaller than those for open β-sheets and β-barrels with shorter strands. The model is reparameterised to account for the reduced twist characteristic of long-stranded transmembrane β-barrels. This produces predictions of both twist and coiling angles that are in agreement with the mean values obtained from the x-ray structures. With the optimized parameters, the model can then be used to determine twist and coiling angles of transmembrane β-barrels from measurements of the amide band infrared dichroism in oriented membranes. Satisfactory agreement is obtained for OmpF. The strand tilt obtained from the x-ray coordinates, or from the reparameterised model, can be combined with infrared dichroism measurements to obtain information on the orientation of the β-barrel assembly in the membrane.

INTRODUCTION

The integral membrane proteins of the porins superfamily and related outer membrane proteins are typified by transmembrane β-sheet barrels in which the axis of the barrel lies preferentially along the membrane normal. The various members of these superfamilies are composed of all next-neighbor anti-parallel strands, but differ in the number of transmembrane β-strands and the stagger between adjacent strands constituting the barrel. The overall configuration of a β-barrel is characterized by the tilt (β) of the strands relative to the barrel axis, the twist (θ) between adjacent strands, and the coiling angle (ϵ) of each strand (Murzin et al., 1994a,b). In the treatment of Murzin et al. (1994a) for idealized regular barrels, these configurational angles are determined uniquely by the number of strands (n) composing the barrel and by the shear number (S) of the barrel, together with an intrinsic tendency of the strands to twist.

The mean tilt angle β of the strands can be determined experimentally for planar β-sheets (Marsh, 1997) and for axially symmetric β-barrels (Marsh, 1998; Tamm and Tatulian, 1997) by means of infrared spectroscopy. This is achieved by combining the dichroic ratios of the amide I and amide II bands that are measured with linearly polarized radiation on aligned samples. Recently, it was shown that the infrared measurements may be extended to derive the twist and coiling of the strands in β-barrel proteins (Marsh, 2000), by using the geometrical formalism of Murzin et al. (1994a).

Here we derive the configurational angles (β, θ, and ϵ) from the crystal coordinates of the members of the outer membrane β-barrel superfamilies. This is useful for several reasons that are connected with both the architecture of protein folding and infrared (IR) analysis of protein orientation in membranes. First, it allows comparison and classification of the growing superfamilies of porin-like structures according to the theoretical treatment of β-barrels by Murzin et al. (1994a,b). Second, it allows comparison of results from infrared spectroscopy with the x-ray structures. Third, it allows one to decide which of the two strategies of infrared analysis currently available (for a planar sheet, or for an axially symmetrical barrel) is more applicable to flattened barrels. Finally, the mean strand tilt determined from the crystal structure can be combined with a single measurement of infrared dichroic ratio (on either the amide I or amide II band) to determine the orientational order parameter of the β-barrel axis in membranes. It is therefore anticipated that the results reported here from the x-ray structures will prove particularly useful for studying β-barrel orientations in membranes by IR methods.

METHODS

β-barrel configuration from x-ray structures

Coordinates of the three-dimensional structures of the different transmembrane β-barrels are taken from the Protein Database (PDB). Local tilt (β_i), twist (θ_i) and coiling (ϵ_i) angles (Fig. 1) are as defined in Murzin et al. (1994a) and also in Marsh (2000). The assignment of families and superfamilies corresponds to that of the SCOP database (Murzin et al., 1995).

The tilt of the β-strands was determined by constructing stepwise the $C^{\alpha,i}$-$C^{\alpha,i+2}$ vectors of the peptide backbone from the x-ray coordinates. The direction taken for all vectors is that from the N- to the C-terminal of the first strand. The scalar product of these vectors with that of the barrel axis

Received for publication 13 December 2000 and in final form 6 March 2001.

Address reprint requests to Dr. Derek Marsh, ABT. 010 Spektroskopie, MPI fuer biophysikalische Chem, Am Fassberg 11, Göttingen, Germany D-37077. Tel: 495512011285; Fax: 495512011501; E-mail: dmarsh@gwdg.de.

© 2001 by the Biophysical Society

0006-3495/01/06/2789/09 $2.00

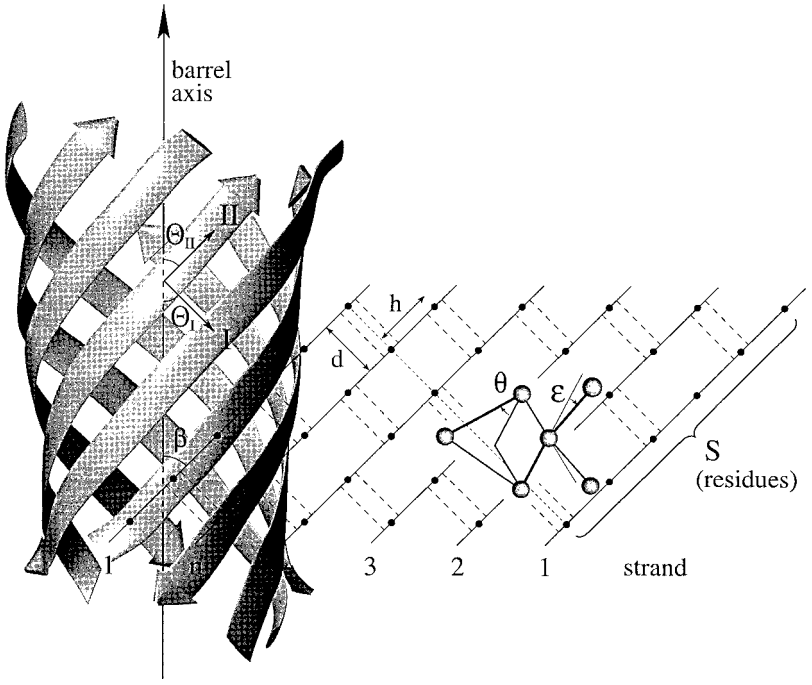

FIGURE 1 Local configurational angles in transmembrane β-barrels. (*Left*) Ribbon plot of the transmembrane section of OmpA (PDB:1QJP; Pautsch and Schulz, 2000). Local vectors parallel to the strand axes are tilted at an angle β to the barrel axis. Transition moments of the amide I and amide II bands are oriented perpendicular and parallel, respectively to the local strand axis. In general, the barrel axis will be oriented at some non-zero angle α to the membrane normal. (*Right*) Schematic topology plot for an n-stranded antiparallel β-barrel. The last strand ($n = 8$ for OmpA) is hydrogen-bonded to the first strand (1). The dotted line traces the residue offset that defines the shear number ($S = 10$ for OmpA). The local sheet twist θ about an axis perpendicular to the strand direction and the local coiling ϵ, along the strands are defined by the (exaggerated) displacement of the residues (*gray circles*) relative to the ideal positions for a planar sheet (*solid dots*).

gives the values of $\cos\beta_i$ that characterize the local strand tilt. The direction of the barrel axis is that closest to the *N*- to C-terminal vector of the first strand, making β_i an acute angle. Summation of $\cos^2 \beta_i$ over all residues, *i*, in the strand, and over all strands in the barrel, was then used to obtain the mean, $\langle\cos^2\beta\rangle$, that determines the infrared dichroism.

For the monomeric porins, the barrel axis was determined by using Insight II (Molecular Simulations Inc., San Diego, CA) with a truncated coordinate set that contained those β-strands forming the barrel. For the trimeric porins, the trimer axis (usually the PDB coordinate *z*-axis) was used for this calculation (Marsh, 1998). Deviations between the monomers of a trimer for which the symmetry axis does not coincide with the crystallographic axis indicate that, where applicable, the uncertainty in orientation of the barrel axis is not $>1°$ for an individual residue. For the mean tilt, the deviations will, to some extent, cancel; this uncertainty does not enter for the twist and coiling angles, which are defined solely in terms of the local axis system. Strands used for the calculation are those identified by the Swiss PDB viewer v.3.5 (Guex and Peitsch, 1997). For calculation of the twist and coiling angles, these were truncated to correspond only to the barrel region.

To determine the mean twist, θ of the β-sheet, a look-up table was first constructed to identify the residues that are in register in adjacent strands. The scalar products of the $C^{\alpha,i}$-$C^{\alpha,i+2}$ vectors corresponding to residues in register were then evaluated stepwise for all adjacent strand pairs. The mean twist was then obtained from the average over all residues and strand pairs. The sign of the twist angle is determined by that of the triple scalar product of the two $C^{\alpha,i}$-$C^{\alpha,i+2}$ vectors with a vector connecting the two strands. The sign convention for θ is that used by Murzin et al. (1994a).

To determine the mean coiling, ϵ, of the strands, the scalar products of the $C^{\alpha,i}$-$C^{\alpha,i+2}$ and $C^{\alpha,i+1}$-$C^{\alpha,i+3}$ vectors were evaluated stepwise for each strand. The value of ϵ was then obtained from the average over all residues and all strands. The sign of the ϵ angle is determined by that of the triple scalar product of the $C^{\alpha,i}$-$C^{\alpha,i+2}$ and $C^{\alpha,i+1}$-$C^{\alpha,i+3}$ vectors with a vector directed along the barrel symmetry axis. The sign convention for ϵ is again that of Murzin et al. (1994a).

Evaluations previously performed by Murzin et al. (1994b) differ only in using strategies that introduce additional smoothing, which could be of advantage for smaller barrels. For the larger transmembrane β-barrels considered here we restrict ourselves to a direct residue-by-residue evaluation, and then simple averaging over all residues, as described above. In the case of strand tilt, this procedure directly reflects the measured IR dichroism.

The above procedures for analyzing the truncated PDB files (i.e., strands-only or barrel-only coordinates) were coded in the PERL programming and scripting language.

Infrared dichroic ratios

The dichroic ratios of the amide infrared bands are determined by the orientation of the vibrational transition moments relative to the alignment axis of the sample. In β-sheets, the resultant transition moments of the amide bands are oriented either parallel (for the amide II) or perpendicular (for the amide I) to the axes of the β-strands (Miyazawa, 1960). For the amide I band, the transition moment therefore makes an angle $\Theta_I = 90\text{-}\beta$ with the β-barrel axis, and correspondingly for the amide II band this angle is $\Theta_{II} = \beta$ (Fig. 1). The other orientational variable that determines the dichroic ratio is then the angle, α, that the β-barrel axis makes with the alignment direction, *z* (e.g., membrane normal). Azimuthal orientation within the plane of the sample is completely random.

For axially symmetric (and monomeric) β-barrels, the orientational variables, β and α, are related to the dichroic ratio, R_z, by (Marsh, 1998; Tamm and Tatulian, 1997):

$$\langle P_2(\cos\Theta_j)\rangle\langle P_2(\cos\alpha)\rangle = \frac{R_z - (E_x^2 + E_z^2)/E_y^2}{R_z - (E_x^2 - 2E_z^2)/E_y^2} \quad (1)$$

where (E_x, E_y, and E_z) are the components of the radiation electric field vector in the sample, relative to those at incidence. The *x* axis lies in the plane of incidence. In Eq. 1, $P_2(x) = \frac{1}{2}(3x^2 - 1)$ is the second order Legendre polynomial, and the angular brackets indicate summations over the corresponding angular distributions. Thus, $<P_2(\cos\alpha)>$ is the order parameter of the β-barrel relative to the director (i.e., membrane normal). For the transition moment orientation, Θ_j, the orientational distribution is that of the (local) strand axes (i.e., of β_i).

Because the β-barrels of several members of the porin family are not axially symmetric, instead are appreciably flattened, Eq. 1 may not be

applicable to analysis of their dichroic ratios. In these cases, the corresponding relations for a planar β-sheet may be more appropriate. These are given by Marsh (1997):

$$\langle\cos^2\Theta_j\rangle\langle\cos^2\alpha\rangle = \frac{R_z - E_x^2/E_y^2}{R_z - (E_x^2 - 2E_z^2)/E_y^2} \qquad (2)$$

where α is the angle that the sheet (equivalent to the barrel axis) makes with the director, and again Θ_j is determined directly by the tilt, β, of the strands within the sheet.

Expressions for the electric field strengths in attenuated total reflection experiments and in transmission experiments at non-zero angles of incidence can be found, for example, in Marsh (1999).

RESULTS AND DISCUSSION

Local configurational angles as a function of sequence position

The dependence on sequence position of the local strand tilt, β_i, the twist, θ_i, and the coiling angle, ϵ_i, is given in Fig. 2 for the small monomeric β-barrel of OmpA (Pautsch and Schulz, 2000). Corresponding data for the larger trimeric β-barrels of the nonspecific porin from *Rhodobacter capsulatus* (Weiss and Schulz, 1992) are given in Fig. 3. The number of data points for twisting and coiling are fewer than for the tilt because a larger number of residues is required to specify the two former angles.

For the eight-stranded β-barrel of OmpA, there is some spread in the local tilt angles, β_i (Fig. 2 *A*). There is also a slight variation in the mean tilt between the different strands, but this is relatively minor. For the 16-stranded nonspecific porin, there is a clear difference in the mean tilt angle between the N-terminal and C-terminal sections of the protein (Fig. 3 *A*). This larger tilt at the trimer interface, compared with the section of the protein facing the lipid, is well-known from the three-dimensional representation of the structure (Weiss and Schulz, 1992). Particularly in the less tilted region exposed to the lipid, the local tilt_i displays remarkably little variation.

The local twist, θ_i, in the OmpA barrel is positive for all except three of the 57 residue positions (Fig. 2 *B*). The

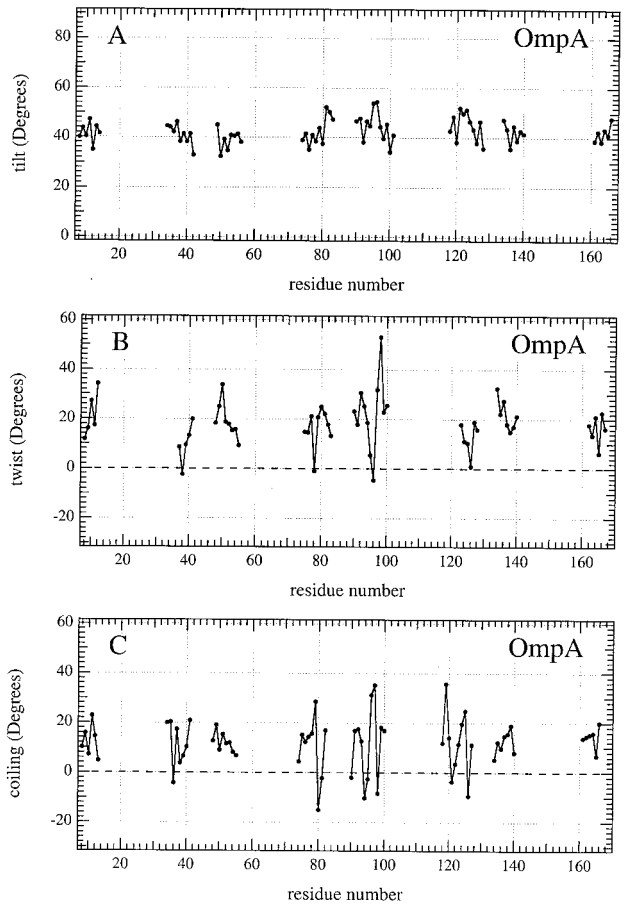

FIGURE 2 Dependence on the residue sequence position of: the local strand tilt, β (*A*); the local sheet twisting, θ (*B*); and the local strand coiling angle, ϵ (*C*) for the monomeric β-barrel of OmpA. Determined using the PDB coordinates 1QJP (Pautsch and Schulz, 2000).

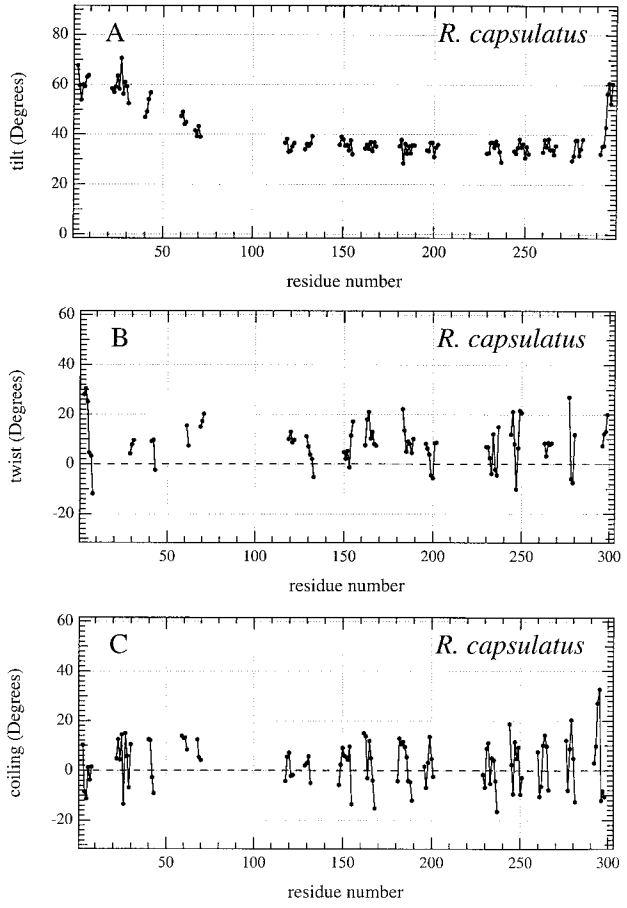

FIGURE 3 Dependence on the residue sequence position of: the local strand tilt, β (*A*); the local sheet twisting, θ (*B*); and the local strand coiling angle, ϵ (*C*) for the trimeric β-barrel of the nonspecific porin from *R. capsulatus*. Determined using the PDB coordinates 2POR (Weiss and Schulz; 1992).

variation in local twist is greatest for one of the strands containing these exceptional residues. In the remaining strands, the mean twist is mostly rather similar. For the larger nonspecific porin, the local twist angle is negative for 12 of 81 residues (Fig. 3 *B*). In certain of the other strands it is almost constant. Overall the twist is distinctly lower than for OmpA. The local coiling angle ϵ_i is more often negative than is the twist angle both for OmpA and for the nonspecific porin (Figs. 2 *C* and 3 *C*). The net coiling angle is, however, considerably larger for OmpA than for the nonspecific porin. To within the local variation, there is little systematic trend in the twist or coiling angles through the sequence. This is in contrast to the behavior of the strand tilt for the nonspecific porin (Fig. 3A).

On the whole, the general features in Figs. 2 and 3 are reasonably representative of these two classes for the whole range of β-barrel structures of the membrane proteins examined. Systematic trends between the different classes of β-barrel membrane proteins are best discerned from the mean values of the configurational angles. This is addressed in the following section.

Average configurational angles from x-ray structures

The mean values of the local strand tilt (β_{eff}) sheet twist, θ, and strand coiling angle, ϵ, are given in Table 1 for all transmembrane β-barrel classes in the protein database. These values are averaged over all residues and all strands, or strand-pairs in the case of the twist angle. The various families are classified according to the number of strands (n) and the shear number (S). For the strand tilt, the effective value (β_{eff}) is obtained from the root-mean-square value of $\cos^2\beta_i$. This is because $\langle\cos^2\beta_i\rangle$ is the quantity determining the infrared dichroism (Eqs. 1 and 2). The mean value of β obtained by directly averaging the values of β_i is almost identical ($\pm$ 0.1°) with the values of β_{eff} given in Table 1, and always within half a degree. The values of β_{eff} given without parentheses in Table 1 cover those sections of the barrel for which the twist and coiling can be determined. This represents a truncation at the ends of the strands, because a larger number of residues is needed to specify the latter two angles. The values of β_{eff} in parentheses are mean values determined from the entire length of all β-strands. This corresponds to the population that determines the infrared dichroic ratio, in the absence of isotopic editing. It also includes any β-strands outside the barrel, particularly those in the cork domain of FhuA (Ferguson et al., 1998) and FepA (Buchanan et al., 1999), and the flag extension of OmpX (Vogt and Schulz, 1999).

Various systematic trends with barrel size and shear numbers are seen in the mean conformational angles given in Table 1. The family of outer membrane proteins consists of two members, OmpX (Vogt and Schulz, 1999) and OmpA (Pautsch and Schulz, 1998; 2000). These have monomeric 8-stranded barrels that differ in their shear numbers. The dependence on shear number is seen clearly in the tilt of the β-strands. The less staggered strands of OmpX are markedly less tilted, the value of β_{eff} being the lowest for all proteins examined. The small number of strands for this family results in a tight radius of curvature. This is reflected in the relatively large twist (and coiling) angles for these proteins, compared with the larger barrels.

The outer membrane phospholipase A2 family has only one representative structure, that of OmpLA (Snijder et al., 1999) and has a 12-stranded barrel with a shear number of 16. This can be considered structurally as a monomer, although the active species is dimeric. The tilt angle is the largest of the proteins examined. This reflects the large

TABLE 1 Mean tilt (β), twist (θ) and coiling (ε) angles of the β-strands in the superfamilies of β-barrel transmembrane proteins

Protein	Ref.*	PDB code	$n^{\ddagger}$	S	β_{eff}(°)†	θ(°)	ε(°)
OmpX	1	1QJ9	8	8	36.2 (36.4)	15.3	8.7
OmpA	2	1QJP	8	10	42.5 (43.1)	18.1	12.0
OmpLA	3	1QD5	12	16	43.4 (46.7)	13.3	5.4
R. caps. porin	4	2POR	16	20	40.8 (42.5)	8.7	2.1
Rps. blastica porin	5	1PRN	16	20	40.4 (42.6)	8.0	5.5
OmpF	6	2OMF	16	20	41.6 (44.8)	7.8	6.1
PhoE	6	1PHO	16	20	41.2 (44.0)	8.9	5.3
OmpK36	7	1OSM	16	20	41.2 (44.5)	8.8	6.1
Lamb	8	1MAL	18	22	41.6 (44.5)	9.4	5.7
Maltoporin	9	2MPR	18	22	40.9 (44.5)	9.3	4.4
ScrY	10	1A0S	18	22	41.1 (43.5)	7.5	4.8
FhuA	11	2FCP	22	24	38.3 (42.4)	6.8	3.5
FepA	12	1FEP	22	24	39.4 (42.2)	6.9	3.8

*References: 1. Vogt and Schulz, 1999; 2. Pautsch and Schulz, 2000; 3. Snijder et al., 1999; 4. Weiss and Schulz, 1992; 5. Kreusch et al., 1994; 6. Cowan et al., 1992; 7. Dutzler et al., 1999; 8. Schirmer et al., 1995; 9. Meyer et al., 1997; 10. Forst et al., 1998; 11. Ferguson et al., 1998; 12. Buchanan et al., 1999.

†Determined from the root-mean-square value of cosβ. Values in parentheses are for all β-strands. All other values are only for strands in the β-barrel.

‡n, number of strands; S, shear number.

TABLE 2 Tilt (β), twist (θ) and coiling (ε) angles for idealised regular β-barrels, with various combinations of *n* and *S*, predicted by Eqs. 3–5*

n	S	β	θ	ε
8	8	35.0°	19.5°	6.7°
8	10	41.2°	18.8°	9.0°
10	12	40.3°	15.0°	7.1°
12	16	43.5°	11.7°	6.8°
14	18	42.5°	10.0°	5.8°
16	20	41.8°	8.7°	5.1°
18	22	41.2°	7.6°	4.5°
20	22	38.2°	6.9°	3.8°
22	24	38.0°	6.2°	3.6°

*Values of $h/d = 0.719$ and $\theta_o = -3.4°$ are used (see text).

shear number ($S - n = 4$) for a relatively small barrel. Also, the twist angle is relatively large for this barrel.

The transmembrane proteins of the porins family all have barrels with 16 strands and a shear number of 20 that are assembled as trimers. This family is represented by five members: the nonspecific porins from *R. capsulatus* (Weiss and Schulz, 1992) and *Rhodopseudomonas blastica* (Kreusch et al., 1994), OmpF and PhoE from *Escherichia coli* (Cowan et al., 1992), and the osmoporin OmpK36 from *Klebsiella pneumoniae* (Dutzler et al., 1999). The mean values of the configurational angles for this family are: $\beta_{eff} = 41.1 \pm 0.5°$ ($43.7 \pm 1.1°$), $\theta = 8.4 \pm 0.5°$, and $\epsilon = 5.0 \pm 1.7°$. This larger barrel is thus characterized by smaller twist and coiling angles than the smaller barrels already considered. The mean tilt is also somewhat smaller than that for OmpA and OmpLA, but this may in part be attributed to heterogeneity in tilt between different strands already discussed (Fig. 3A).

The maltoporin-like family is represented by three members: Lamb from *E. coli* (Dutzler et al., 1995; Schirmer et al., 1995; Wang et al., 1997), and maltoporin (Meyer et al., 1997) and the sucrose specific porin ScrY (Forst et al., 1998) from *Salmonella typhimurium*. This family has trimerically assembled barrels that have 18 strands with a shear number of 22. The mean values of the configurational angles are: $\beta_{eff} = 41.2 \pm 0.4°$ ($44.2 \pm 0.6°$), $\theta = 8.7 \pm 1.1°$ and $\epsilon = 5.0 \pm 0.7°$. These values are rather similar to those for the porins family of which the structures are also trimeric and have a value of $S - n = 4$.

Finally, the family of ligand-gated protein channels has two representative structures: those of the Fe-siderophore active transporters FhuA (Ferguson et al., 1998; Locher et al., 1998) and FepA (Buchanan et al., 1999), both from *E. coli*. These are the largest barrels for which the structure has been determined to date. They consist of 22 strands with a shear number of 24 and are monomeric. The mean configurational angles are rather similar for FepA and FhuA and are reduced relative to those of the medium-sized barrels of the trimeric nonspecific porin and maltoporin-like families.

Comparison with idealized regular barrels

Infrared dichroism from non-isotopically edited β-barrels provides an average over all β-strand residues (Eqs. 1 and 2). Therefore it is useful to test to what extent the mean values of the configurational angles given in Table 1 conform to those of an equivalent idealized regular β-barrel. The systematic trends that are found with barrel size and shear number in Table 1 indicate that this may be a viable approach. In a regular symmetrical barrel, the β-strand configuration is determined by the number of strands and the shear number, together with the intrinsic tendency of the β-sheets to twist (McLachlan, 1979; Murzin et al., 1994a). The principal reason for attempting to establish this correspondence is that the infrared dichroic ratios may then be used to estimate the mean twist and coiling angles in the β-barrel (Marsh, 2000).

The tilt β, of the β-strands relative to the β-barrel axis is given by (Chou et al., 1990; McLachlan, 1979)

$$\tan\beta = \frac{h}{d}\frac{\sin(\pi/n)}{\pi} S \tag{3}$$

where h is the rise per residue along the strand and d is the separation between adjacent strands (Fig. 1). For the antiparallel β-sheet of β-poly-L-alanine: $h/d = 0.729$ as deduced from refined coordinates (Arnott et al., 1967). Fitting Eq. 3 to the data for β_{eff} in Table 1 with h/d as the only adjustable parameter yields a value of $h/d = 0.719 \pm 0.022$. This lies close to the value from direct determinations of h and d that was just quoted. Eq. 3 therefore provides a reasonable representation of the mean strand tilts in the x-ray structures of the β-barrel proteins from Table 1. Values of β, calculated from Eq. 3 with the optimized value of $h/d = 0.719$, are given in Table 2, for various combinations of n and S.

Comparison of the predictions in Table 2 with the values of the mean tilt angle obtained from the x-ray structures in Table 1 shows reasonable quantitative agreement. Differences between the experimental values and the predictions for a regular symmetrical barrel are ~1°, when averages are taken over structures with the same n and S. Although relatively small, the deviations between predicted and observed values are consistently negative for the monomeric barrels and positive for the trimeric barrels. Overall, these results suggest that Eq. 3 with $h/d = 0.719$ may be used with reasonable confidence to predict the average strand tilt for transmembrane β-barrels of unknown structure. Some such predictions are included in Table 2. Greater precision might be achieved by using separately optimized values of h/d for monomeric ($h/d = 0.739 \pm 0.017$) and trimeric ($h/d = 0.708 \pm 0.013$) barrels.

The twist, θ, of the β-strands for an ideal regular β-barrel is obtained in the model of Murzin et al. (1994a) by minimizing the free energy of twisting and coiling for parabolic deviations about the most favourable value, θ_o, of the twist

in an unstrained sheet. The optimized value of the twist in an idealized regular barrel is then given by Marsh (2000):

$$\theta = \frac{\theta_o + 2\pi(h/d)(n/S + S/n)/\sqrt{(h/d)^2S^2 + n^2}}{1 + n^2/S^2 + (h/d)^2S^2/n^2} \quad (4)$$

where an approximation is used that sines of half-angles are replaced by their arguments (in radians). In their original analysis, Murzin et al. (1994a) took $\theta_o = 20°$, which corresponds to the mean twist in open sheets that are not constrained to form a barrel and in which the strands are relatively short (Chothia and Janin, 1981; Janin and Chothia, 1980). Using this value of θ_o, the values of θ predicted from Eq. 4 are uniformly larger than the observed values given in Table 1. However, as pointed out by Murzin et al. (1994b), long strands cannot support a large twist if they are to stay within hydrogen bonding distance of the adjacent strands along their entire length. Transmembrane β-barrels are characterized by long strands, typically of 9 residues or more, in order to span the membrane. To allow for this it is necessary to take a smaller value of θ_o. Fitting Eq. 4 to the data for θ given in Table 1 with $h/d = 0.719$, as obtained above, and θ_o as the only adjustable parameter yields a value of $\theta_o = -3.4 \pm 3.9°$. The values of θ obtained from Eq. 4 by using this value of θ_o are given in Table 2, for various combinations of n and S.

Comparison of the predictions in Table 2 with the observed average values of θ in Table 1 reveals that the predictions are reasonably successful for the larger barrels which have relatively small twists, but less good for the smallest barrel OmpX. This most likely reflects the fact that barrels with smaller numbers of strands are more sensitive to distortions from axial symmetry. For OmpA, which is the most symmetrical of the smaller barrels, the prediction is quite good.

The coiling angle, ϵ, of the β-strands in an ideal regular β-barrel is related geometrically to the twist angle, θ (Murzin et al., 1994a). The relation in terms of n, S, and $\theta(n, S)$ is given by Marsh (2000):

$$\varepsilon = \frac{2\pi(h/d)}{\sqrt{(h/d)^2 S^2 + n^2}} - \frac{n}{S}\,\theta(n, S) \quad (5)$$

where $\theta(n, S)$ is obtained from Eq. 4. Again, the approximation for the sines of half-angles is used. The values of the coiling angle predicted by Eq. 5 are given in Table 2, for a range of values of n and S. Values of $h/d = 0.719$ and $\theta_o = -3.4°$ established above were used in these calculations, without any further adjustments. Comparison with the experimental values of ϵ given in Table 1 shows that the observed trend is reproduced very well. Also, the absolute values are reasonably close, when values with the same n and S are averaged. The largest difference is again obtained for the smaller barrels with deviations of 1–3° for OmpX, OmpA and OmpLA. All other values are very similar, when averaged over barrels with the same n and S.

Experimental infrared dichroic ratios

Infrared transmission data has been determined for the amide I and amide II bands of OmpF in oriented membranes (Nabedryk et al., 1988). The dichroic ratios measured for the two bands may be combined to give separately the tilt, β, of the strands and the distribution in tilt, α, of the sheet/barrel axis (Marsh, 1999). The experimental value for the mean strand tilt is characterized by a value of $<P_2(\cos\beta)> = 0.28$ assuming an axially symmetrical β-barrel (i.e., using Eq. 1), and by a value of $<P_2(\cos\beta)> = 0.27$ assuming a planar β-sheet (i.e., using Eq. 2). The corresponding value deduced from the crystal structure is $<P_2(\cos\beta)> = 0.26$ using the value of β_{eff} for all strands (Table 1), in reasonable agreement with the infrared values. The average value of $\langle P_2(\cos\beta)\rangle$ derived from the amide dichroic ratios corresponds to an effective mean strand tilt of $\beta_{eff} = 44.1°$. This may then be used, together with the expressions given in Marsh (2000), to obtain values for the twist and coiling of the β-strands. With $h/d = 0.719$ and $\theta_o = -3.4°$ the resulting values are $\theta = 8.4°$ and $\epsilon = 5.4°$, respectively. These are within 1° of the values obtained from the x-ray structure of OmpF that are given in Table 1.

The β-barrel of OmpF is rather large in cross-section and, more importantly, is considerably flattened. Also, the trimeric structure of OmpF potentially can contribute to the non-axiality (Marsh, 1998). Therefore it is likely that the dichroic ratios might be biased in the direction expected from a planar sheet analysis relative to that for an axially symmetric barrel. This is indeed what is found (see above). For OmpF the infrared values of strand tilt specified by $\langle P_2(\cos\beta)\rangle$ are, however, still rather similar using both methods of analysis. Nevertheless, distinction between the two models is important because they yield different values for the order parameter, $\langle P_2(\cos\alpha)\rangle$, of the barrel/sheet assembly relative to the membrane normal (Eqs. 1 and 2, respectively). Using the β-barrel analysis a value of $\langle P_2(\cos\alpha)\rangle = 0.69$ is obtained as compared with $\langle P_2(\cos\alpha)\rangle = 0.84$ from the β-sheet analysis. The true value will lie between these two extremes. In cases for which the two methods of analysis yield more divergent values of $\langle P_2(\cos\beta)\rangle$, the value obtained from the x-ray structure becomes important in deciding which model is the more appropriate. Then the order parameter of the barrel axis in the membrane can be obtained from the corresponding infrared measurements. (Note that the azimuthal orientation in the membrane plane does not enter into a conventional dichroism experiment because the sample is rotationally disordered.)

An alternative method of analysis is to combine the value of the strand tilt from the x-ray structure with the dichroic ratios from infrared measurements. This then

again gives the order parameter of the β-barrel in the membrane. For OmpF, this gives values of $\langle P_2(\cos\alpha)\rangle = 0.69 \pm 0.06$ using the β-barrel analysis and $\langle P_2(\cos\alpha)\rangle = 0.84 \pm 0.03$ from the formalism appropriate to β-sheets. The range of uncertainty corresponds to values obtained by using the amide I and amide II dichroic ratios, respectively. Better agreement between the two is obtained with the β-sheet formalism, as expected because this yields a mean strand tilt closer to that found from the x-ray structure. Use of data from the x-ray structure (or failing that predictions for idealized symmetrical barrels) should be particularly valuable when only one infrared dichroic ratio is available. Attenuated total reflection measurements on the amide I band of OmpA (Rodianova et al., 1995) are a possible case in point. The consistency of the two methods of analysis that was obtained for OmpF indicates that this should also be a reliable approach to determining the orientation of the β-barrel in the membrane. The values of β_{eff} reported in Table 1 should be especially useful in this respect.

It should be noted that the value determined for the orientation, α, of the barrel axis (but not that for the strand β) tilt, depends on the degree of alignment of the sample (Rothschild and Clark, 1979). With suitable techniques for sample preparation, high degrees of alignment can be obtained for IR studies (Clark et al., 1980).

The above example illustrates how the configurational data from x-ray structures can help in using infrared dichroism measurements to obtain information on the orientation of the protein in its membrane environment. In the absence of x-ray structures, the comparison between Tables 1 and 2 indicates that Eq. 3 together with the value of h/d optimized on the database for transmembrane β-barrels may be used instead as a suitable approximation.

CONCLUSIONS

Analysis of the x-ray structures for transmembrane β-barrels (Table 1) reveals that for all except the smaller β-barrels of OmpX, OmpA, and OmpLA, the mean twist angles are less than those found for the unconstrained open β-sheets in soluble proteins. For the latter, a mean twist angle of $\sim$19° is found with α/β folds (Janin and Chothia, 1980) and 17° for the aligned class in which the sheets pack face-to-face (Chothia and Janin, 1981). For OmpX, OmpA and OmpLA, the twist angles are comparable to these latter values (average $\theta = 16° \pm 2°$), but for the remainder the average twist is $\theta = 8° \pm 1°$. This is in contrast to the situation for the shorter β-barrels in soluble proteins, where the twist angle is greater than for open β-sheets and has an average value of $32° \pm 7°$ (Murzin et al., 1994b).

As already explained, this is because transmembrane β-barrels of necessity contain long β-strands. Also, the hydrophobic membrane environment dictates that all peptide hydrogen bonds must be satisfied within the β-sheet. A consequence of this is that a smaller value of θ_o than for shorter barrels is required to describe the dependence of the twist angle on the number of strands and the shear number by means of Eq. 4. The model of Murzin et al. (1994a) then fits both the observed mean twist angles and the observed mean coiling angles reasonably well (compare Tables 1 and 2). For reference, the dependence of the configurational angles on n and S that is predicted by Eqs. 3–5 with the values $h/d = 0.719$ and $\theta_o = -3.4°$ derived here for transmembrane β-barrels is given in the Appendix. It is seen there that the predictions for an idealized symmetrical barrel reproduce the trends with n and S that are found in Table 1 for transmembrane β-barrels.

The mean coiling angles, ϵ, of the transmembrane β-barrels are all positive and greater than zero (average $\epsilon = 6 \pm 2°$). This is in contrast to the situation for open β-sheets in soluble proteins, where the coiling may take either positive or negative values, with a mean close to zero for sheets with short strands (Baker and Hubbard, 1984; Murzin et al., 1994a). For the shorter β-barrels in soluble proteins, on the other hand, the coiling angles are almost exclusively positive, with a mean value of $\epsilon = 7 \pm 5°$ (Murzin et al., 1994b). This is not very dissimilar to the situation for transmembrane β-barrels.

The values of $h/d = 0.719$ and $7\theta_o = -3.4°$ optimized here for transmembrane β-barrels may be used with some confidence to determine the mean twist and coiling angles from the mean strand tilt obtained in infrared dichroism experiments on this class of membrane-bound proteins (Marsh, 2000). Analysis of the x-ray coordinates, together with the infrared dichroism of β-barrel transmembrane proteins, also allows determination of the orientation (or order parameter) of the β-barrel in the membrane. Obviously, this is a quantity that cannot be obtained from the crystal structure. For flattened β-barrel structures, e.g., OmpF, determination of the mean strand tilt from the x-ray structure is necessary to decide whether the planar sheet or axially symmetric barrel model is best suited to interpret the infrared data. For axially symmetric barrels, e.g., OmpA, this is also necessary if dichroic ratios are measured only for the amide I band. The values of β_{eff} in Table 1 would then be combined directly with the IR measurements.

APPENDIX

Configurational angles for an ideal, regular β-barrel

The dependence of the strand tilt angle, β, on shear number, S, that is predicted by Eq. 3 is given for barrels with different (even) numbers of strands, n, in Fig. 4 . Correspondingly, the dependence of the sheet twist angle, θ, on shear number that is predicted from Eq. 4 is given in Fig. 5 for barrels with different numbers of strands. Finally, the dependence of the

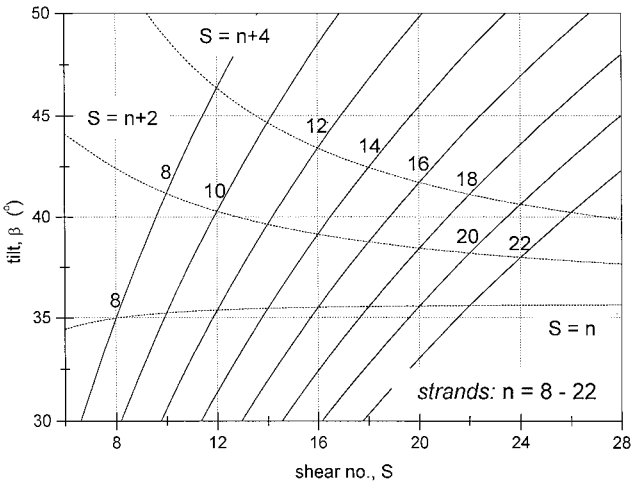

FIGURE 4 Dependence on shear number, S, of the tilt, β, of the β-strands, relative to the barrel axis, for regular idealized β-barrels that is given by Eq. 3. The solid lines are for barrels with $n = 8$, 10, 12, 14, 16, 18, 20, and 22 strands (from *top* to *bottom*, respectively). The dotted lines are for barrels with shear numbers: $S = n + 4$, $n + 2$ and n (from *top* to *bottom*, respectively). Figures given at the intersections of the solid and dotted curves correspond to values of n for the combinations of n and S that are given in Table 2.

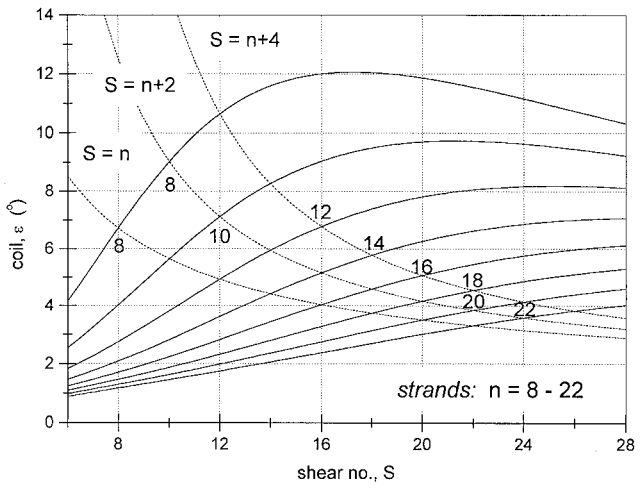

FIGURE 6 Dependence on shear number, S, of the coiling angle, ϵ, of the β-strands in regular idealized β-barrels that is given by Eqs. 4 and 5. The solid lines are for barrels with $n = 8$, 10, 12, 14, 16, 18, 20, and 22 strands (from *top* to *bottom* at the *right* ordinate, respectively). The dotted lines are for barrels with shear numbers $S = n + 4$, $n + 2$ and n (from *top* to *bottom*, respectively). Values of n given at the intersections of the solid and dotted curves are for barrels with shear numbers given in Table 2.

coiling angle, ϵ, on shear number that is predicted by Eqs. 4 and 5 for barrels with various numbers of strands is given in Fig. 6. In all these calculations, values of $h/d = 0.719$ and $\theta_o = -3.4°$ that were optimized for transmembrane β-barrels are used.

The increase in strand tilt with increasing shear number, i.e., with increasing stagger between adjacent strands, is seen clearly in Fig. 4 (solid lines). For barrels with fixed n, the effect is greater the smaller the number of strands. This dependence is seen very clearly for OmpX and OmpA in Table 1. The tilt increases with decreasing n, the effect being larger for smaller barrels. For barrels with a fixed value of $S - n > 0$, the tilt angle decreases with increasing n, but the effect becomes small for the larger barrels. This trend is found in comparing OmpA with FhuA and FepA or OmpLA with the porins in Table 1, but less clearly in comparing the porins with the maltoporins where n is large and differs only by two strands.

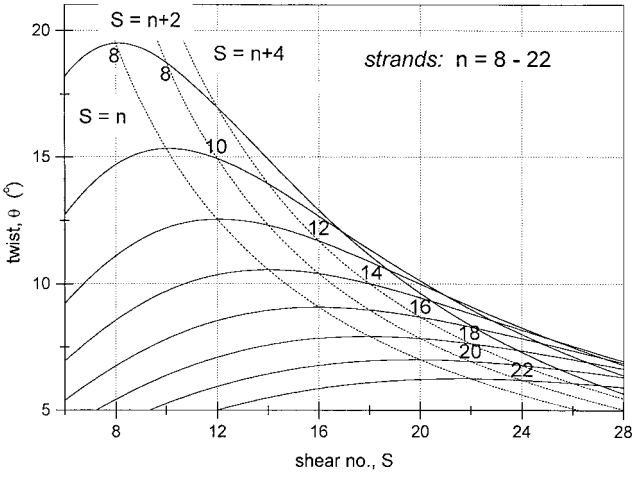

FIGURE 5 Dependence on shear number, S, of the twist, θ, of the β-strands in regular idealized β-barrels that is given by Eq. 4. The solid lines are for barrels with $n = 8$, 10, 12, 14, 16, 18, 20, and 22 strands (from *top* to *bottom* at the *left* ordinate, respectively). The dotted lines are for barrels with shear numbers $S = n+4$, $n+2$ and n (from *top* to *bottom*, respectively). Values of n given at the intersections of the solid and dotted curves are for the combinations of n and S given in Table 2.

The dependence of the twist angle on shear number is non-monotonic (Fig. 5). In principle, this might explain why θ is smaller for OmpX than for OmpA, although with $\theta_o = -3.4°$ OmpX is predicted to have the maximum value of θ. For shear numbers of $S = n$ and greater (with $\theta_o = -3.4°$), the twist angle decreases with increasing shear number, for fixed n. For shear numbers $S = n$ to $S = n + 4$, the twist angle decreases with increasing n, the decrease being greatest for the smaller barrels. This effect is found in the observed values of θ for OmpA and FhuA or FepA, and for OmpLA compared with the porins and maltoporins, in Table 1.

The dependence of the coiling angle on shear number is, again, biphasic, but for the region of interest, ϵ always increases with increasing shear number and fixed n. This is in contrast to the behavior of the twist angle, but more similar to that of the strand tilt. This predicted increase is seen very clearly in the observed values of ϵ for OmpX and OmpA (Table 1). For shear numbers $S = n$ to $S = n + 4$, the coiling angle decreases with increasing n, although the dependence becomes relatively small for larger barrels. Again this prediction holds for the observed values of ϵ in Table 1. The coiling angle decreases strongly between OmpA and FhuA or FepA, but less strongly between OmpLA and the porins or maltoporins.

REFERENCES

Arnott, S., S. D. Dover, and A. Elliot. 1967. Structure of β-poly-L-alanine: Refined atomic co-ordinates for an anti-parallel beta-pleated sheet. *J. Mol. Biol.* 30:201–208.

Baker, E. N., and R. E. Hubbard. 1984. Hydrogen bonding in globular proteins. *Prog. Biophys. Mol. Biol.* 44:97–179.

Buchanan, S. K., B. S. Smith, L. Venkatramani, D. Xia, L. Esser, M. Palnitkar, R. Chakraborty, D. van der Helm, and J. Deisenhofer. 1999. Crystal structure of the outer membrane active transporter FepA from *Escherichia coli*. *Nat. Struct. Biol.* 6:56–63.

Chothia, C., and J. Janin. 1981. Relative orientation of close-packed β-pleated sheets in proteins. *Proc. Natl. Acad. Sci. U.S.A.* 78: 4146–4150.

Chou, K.-C., L. Carlacci, and G. G. Maggiora. 1990. Conformational and geometrical properties of idealized β-barrels in proteins. *J. Mol. Biol.* 213:315–326.

Clark, N. A., K. J. Rothschild, D. A. Luippold, and B. A. Simon. 1980. Surface-induced lamellar orientation of multilayer membrane arrays. Theoretical analysis and a new method with application to purple membrane fragments. *Biophys. J.* 31:65–96.

Cowan, S. W., T. Schirmer, G. Rummel, M. Steiert, R. Ghosh, R. A. Pauptit, J. N. Jansonius, and J. P. Rosenbusch. 1992. Crystal structures explain functional properties of two *E. coli* porins. *Nature.* 358:727–733.

Dutzler, R., G. Rummel, S. Alberti, S. Hernández-Allés, P. S. Phale, J. P. Rosenbusch, V. J. Benedi, and T. Schirmer. 1999. Crystal structure and functional characterization of OmpK36, the osmoporin of *Klebsiella pneumoniae*. *Structure.* 7:425–434.

Dutzler, R., Y.-F. Wang, P. J. Rizkallah, J. P. Rosenbusch, and T. Schirmer. 1995. Crystal structures of various maltooligosaccharides bound to maltoporin reveal a specific sugar translocation pathway. *Structure.* 4:127–134.

Ferguson, A. D., E. Hofmann, J. W. Coulton, K. Diederichs, and W. Welte. 1998. Siderophore-mediated iron transport: crystal structure of FhuA with bound lipopolysaccharide. *Science.* 282:2215–2220.

Forst, D., W. Welte, T. Wacker, and K. Diederichs. 1998. Structure of the sucrose-specific porin ScrY from *Salmonella typhimurium* and its complex with sucrose. *Nat. Struct. Biol.* 5:37–46.

Guex, N., and M. C. Peitsch. 1997. Swiss Model and the Swiss-Pdb Viewer: An environment for comparative protein modeling. *Electrophoresis.* 18:2714–2723.

Janin, J., and C. Chothia. 1980. Packing of α-helices onto β-pleated sheets and the anatomy of α/β proteins. *J. Mol. Biol.* 143:95–128.

Kreusch, A., A. Neubüser, E. Schiltz, J. Weckesser, and G. E. Schulz. 1994. Structure of the membrane channel porin from *Rhodopseudomonas blastica* at 2.0 Å resolution. *Prot. Science.* 3:58–63.

Locher, K. P., B. Rees, R. Koebnik, A. Mitschler, L. Moulinier, J. P. Rosenbusch, and D. Moras. 1998. Transmembrane signaling across the ligand-gated FhuA receptor: crystal structures of free and ferrichrome-bound states reveal allosteric changes. *Cell.* 95:771–778.

Marsh, D. 1997. Dichroic ratios in polarized Fourier transform infrared for nonaxial symmetry of β-sheet structures. *Biophys. J.* 72:2710–2718.

Marsh, D. 1998. Nonaxiality in infrared dichroic ratios of polytopic transmembrane proteins. *Biophys. J.* 75:354–358.

Marsh, D. 1999. Spin label ESR spectroscopy and FTIR spectroscopy for structural/dynamic measurements on ion channels. *Methods Enzymol.* 294:59–92.

Marsh, D. 2000. Infrared dichroism of twisted β-sheet barrels. The structure of *E. coli* outer membrane proteins. *J. Mol. Biol.* 297:803–808.

McLachlan, A. D. 1979. Gene duplications in the structural evolution of chymotrypsin. *J. Mol. Biol.* 128:49–79.

Meyer, J. E. W., M. Hofnung, and G. E. Schulz. 1997. Structure of maltoporin from *Salmonella typhimurium* ligated with a nitrophenyl-maltotrioside. *J. Mol. Biol.* 266:761–775.

Miyazawa, T. 1960. Perturbation treatment of the characteristic vibrations of polypeptide chains in various configurations. *J. Chem. Phys.* 32: 1647–1652.

Murzin, A. G., S. E. Brenner, T. Hubbard, and C. Chothia. 1995. SCOP - a structural classification of proteins database for the investigation of sequences and structures. *J. Mol. Biol.* 247:536–540.

Murzin, A. G., A. M. Lesk, and C. Chothia. 1994a. Principles determining the structure of β-sheet barrels in proteins. I. A theoretical analysis. *J. Mol. Biol.* 236:1369–1381.

Murzin, A. G., A. M. Lesk, and C. Chothia. 1994b. Principles determining the structure of β-sheet barrels in protein. II. The observed structures. *J. Mol. Biol.* 236:1382–1400.

Nabedryk, E., R. M. Garavito, and J. Breton. 1988. The orientation of β-sheets in porin. A polarized Fourier transform infrared spectroscopic investigation. *Biophys. J.* 53:671–676.

Pautsch, A., and G. E. Schulz. 2000. High-resolution structure of the OmpA membrane domain. *J. Mol. Biol.* 298:273–282.

Rodianova, N. A., S. A. Tatulian, T. Surrey, F. Jähnig, and L. K. Tamm. 1995. Characterization of two membrane-bound forms of OmpA. *Biochemistry.* 34:1921–1929.

Rothschild, K. J., and N. A. Clark. 1979. Polarized infrared spectroscopy of oriented purple membrane. *Biophys. J.* 25:473–488.

Schirmer, T., T. A. Keller, Y.-F. Wang, and J. P. Rosenbusch. 1995. Structural basis for sugar translocation through maltoporin channels at 3.1 Å resolution. *Science.* 267:512–514.

Snijder, H. J., I. Ubarretxena-Belandia, M. Blaauw, K. H. Kalk, H. M. Verheij, M. R. Egmond, N. Dekker, and B. W. Dijkstra. 1999. Structural evidence for dimerization-regulated activation of an integral membrane phospholipase. *Nature.* 401:717–721.

Tamm, L. K., and S. A. Tatulian. 1997. Infrared spectroscopy of proteins and peptides in lipid bilayers. *Q. Rev. Biophys.* 30:365–429.

Vogt, J., and G. E. Schulz. 1999. The structure of outer membrane protein OmpX from *Escherichia coli* reveals possible mechanisms of virulence. *Struct. Fold. Des.* 7:1301–1309.

Wang, Y.-F., R. Dutzler, P. J. Rizkallah, J. P. Rosenbusch, and T. Schirmer. 1997. Channel specificity: structural basis for sugar discrimination and differential flux rates in maltoporin. *J. Mol. Biol.* 272: 56–63.

Weiss, M. S., and G. E. Schulz. 1992. Structure of porin refined at 1.8 Å resolution. *J. Mol. Biol.* 227:493–509.